DNA nanostructures based biosensor for the determination of aromatic compounds

S Baby Gayathri, P Kamaraj, M Arthanareeswari, S Devikala

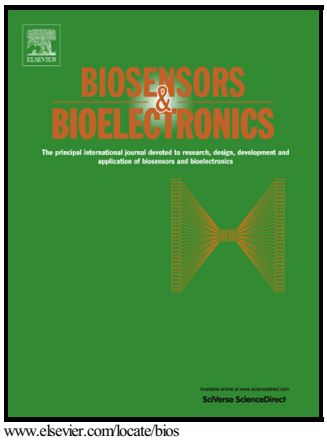

www.elsevier.com/locate/bios

PII: S0956-5663(15)30099-3
DOI: http://dx.doi.org/10.1016/j.bios.2015.05.002
Reference: BIOS7664

To appear in: *Biosensors and Bioelectronic*

Received date: 14 March 2015
Revised date: 30 April 2015
Accepted date: 3 May 2015

Cite this article as: S Baby Gayathri, P Kamaraj, M Arthanareeswari and S Devikala, DNA nanostructures based biosensor for the determination of aromatic compounds, *Biosensors and Bioelectronic,* http://dx.doi.org/10.1016/j.bios.2015.05.002

DNA nanostructures based biosensor for the determination of aromatic compounds

S Baby Gayathri, P Kamaraj, M Arthanareeswari, S Devikala.*

Department of Chemistry, SRM University, Kattankulathur 603203, India.

Phone: +91-9962510141; e-mail: babygayathri@gmail.com

ABSTRACT

Graphite electrode was modified using multi-walled carbon nanotubes (MWCNT), chitosan (CS), glutaraldehyde (GTA) and DNA nanostructures. DNA nanostructures (nsDNA) of 50 nm in size were produced from single DNA template sequence using a simple two step procedure and were confirmed using TEM and AFM analysis. The modified electrode was applied to the electrochemical detection of aromatic compounds using EIS. The modified electrode was characterized using differential pulse voltammetry (DPV), electrochemical impedance spectroscopy (EIS) and cyclic voltammetry (CV). For comparison, electrochemical results derived from single stranded (50 bp length) and double stranded (50bp length) DNA based biosensors were used. The results indicate that the modified electrode prior to nsDNA immobilization provides a viable platform that effectively promotes electron transfer between nsDNA and the electrode. The mode of binding between the nsDNA and aromatic compounds was investigated using EIS, indicating that the dominant interaction is non-covalent. nsDNA based biosensor was observed to act as an efficient biosensor in selective and sensitive identification of aromatic compounds.

Keywords: aromatic compounds, biosensor, DNA nanostructures, multi-walled carbon nanotubes, electrochemical characterization, electrochemical impedance spectroscopy.

1. Introduction

Initially, studies on the application of DNA in biosensor were conducted in order to achieve a high sensitive, cost effective and quantitative feature for the detection of specific gene. Later in 1988, Palecek demonstrated the behavior of nucleic acids producing a well developed voltammetric peaks on mercury electrode. Later a small damage in double helical DNA was also electrochemically identified (Palecek, 1996). Since then, several polarographic and voltammetric

methods have been proposed for the direct quantification of nucleic acids, for the detection of hybridization and for the evaluation of DNA damage (Gayathri and Kamaraj, 2015). The reported applications involve the determination of electroactive and non-electroactive compounds interacting with DNA, detection of specific sequence of DNA and monitoring DNA integrity (Kamel et al., 2008).

When nucleic acids encounter a toxin or aromatic compounds, DNA damage occurs which will be reflected in the change in oxidation signal of purine bases. Most of the available literature have used calf thymus or herring sperm DNA in biosensor for the detection of different environmental contaminants such as Polychlorinated biphenyl (PCB) mixtures, atrazine, phthalate, hydrazine, (Marrazza et al., 1999) aromatic amines and polycyclic aromatic hydrocarbon (PAH) (Carlo et al., 2008). In all the studies, either the single stranded, or double stranded or both of the DNA have been used. It was inferred that the ssDNA immobilized electrode shows a higher oxidation signal in comparison with dsDNA, as the bases in the ssDNA are free to react with the neighbouring molecules. It should be noted that the use of ss or dsDNA lacks selectivity in the identification of toxins or chemical compounds. In this report, the authors demonstrate the construction of DNA nanostructure, its electrochemical properties and its possible application for the selective identification of aromatic compounds.

DNA nanotechnology utilizes the unique molecular recognition properties of nucleic acids to create self-assembling DNA complexes at the nanoscale termed as nanostructured DNA. Here, DNA is used as structural material rather than a carrier of biological codes. DNA is known to form an ordered self assembled structure through bottom up approach (Pelesko, 2007). By understanding the chemistry behind the DNA stability, it is possible to obtain DNA nanostructures in the form of cubes, polyhydra, tiles, bare code etc. The literatures on the stability of DNA have paved way for easy design of the DNA sequence to construct DNA nanostructures.

2. Materials and Methods

2.1. Materials used:

All the electrochemical measurements were recorded using the instrument SP-300 from Biologic Science Instrument, France, running on EC-Lab Software (Version 10.18) and with standard calomel electrode as reference electrode, platinum wire as counter electrode and graphite electrode (surface area = 0.318 cm^2) as working electrode. Calomel electrode used in

this experiment has 0.241V (electrode surface area= 0.001cm^2) as offset potential against normal hydrogen electrode. All the electrochemical measurements were made using 20ml cell containing 15ml of supporting electrolyte.

Graphite rods were purchased from HomeScience Tools, Montana, USA. The procured rods were cut into 5 equal sizes and rubbed over micro alumina powder for several minutes until a smooth surface of diameter 0.636cm was obtained. In order to make electrical contact, conducting wires of equal length were pasted at the side of the sliced graphite rods using silver paste. It was then coated with Teflon leaving the bottom surface for it to act as sensor after modifications. MWCNT of (30±15) nm diameter and length of several microns were obtained from Applied Science Innovation Pvt. Ltd, Maharashtra, India. MWCNTs were oxidized using concentrated nitric acid by sonicating it for 30 minutes, in order to remove impurities. After which, the suspension was washed several times with water to remove trace amount of nitric acid in the nanotubes. Mono sodium phosphate and di-sodium phosphate were obtained from Merck, NJ, USA. Double distilled water was used throughout the experiment. All other chemicals were obtained from Sisco Research Laboratories and were used without any further purification. Solutions of aromatic compounds were prepared immediately before each experiment.

DPV measurements were carried out in 0.1M Phosphate buffer. CV and EIS measurements were made in 0.1M NaCl solution containing 10/10mM $K_3Fe(CN)_6/K_4Fe(CN)_6$. The DNA template sequence nsDNA nanostructures were manually designed and purchased from Sigma Aldrich, Mumbai, India as follows:

nsDNA template:

5'GCACGAGTCCTAACGCTGTGCGTTAGGTGATACCGAGACGGTATACGGCTTACGTGTCG TAAGCCACTCGTGC3'

2.2. Designing of DNA nanostructures:

The melting temperature of the designed sequence was calculated to be 72.3 ºC with 56.2% of GC rich regions. The template was so designed that it forms four self-dimers, three hairpin loops, and one Holliday junction.

The protocol for the preparation of DNA nanostructures are as follows:

Step 1: Annealing at 90 ºC for 2 minutes

Step 2: Hairpin formation at 58 ºC for 30 minutes

Step 3: Cooling at 4 ºC

Transmission Electron Microscope (TEM) and Atomic Force Microscope (AFM) were used to confirm the formation of DNA nanostructure.

2.3. Preparation of DNA nanostructure based biosensor

The immobilization of DNA at an electrode surface is a crucial aspect to develop DNA biosensors for monitoring analyte interactions. Immobilization of DNA is the primary step responsible for the accessibility of a given molecule in solution to the confined DNA and hence, it will influence the affinity of analyte binding. The key criterion for a successful DNA immobilization is to keep the DNA bases accessible to the binding of target molecules present in solution (Arias et al., 2009). There are many reported methods for surface-immobilization of ssDNA on electrodes such as chemical adsorption, covalent-binding, antigen-antibody method, electrostatic attraction and co-polymerization (Cai et al., 2001). In this report, electrostatic attraction method has been used for the immobilization of over the modified graphite electrode.

1 gm of oxidized MWCNTs was dispersed in 1 ml of 1 % V/V acetic acid solution containing 0.5 mg of chitosan by sonication for 30 minutes. 30 µl of the prepared CS-MWCNT gel was dropped on the surface of the cleaned graphite electrode and dried at room temperature to form CS-MWCNT nanocomposite film on the electrode surface. The resulting electrode was named as CS-MWNT/G. This electrode was then washed with double distilled water and immersed into the solution containing 1 % glutaraldehyde for 2 hours to obtain GTA/CS-MWCNT/G electrode which can be stored at 4 °C for further analysis. This electrode can be reused by rubbing it over 0.05 µm alumina slurry until a smooth polished surface is obtained.

The stock solution of the nsDNA primers were heated to its annealing temperature and slowly cooled thereafter using thermal cycler in order to form the hairpin bends as expected upon cooling at 58 ºC. nsDNA/GTA/CS-MWCNT/G electrode was developed by immobilizing 60 mg/l of heat treated nsDNA at a fixed potential (+0.3 V versus Calomel/Platinum electrode for 180 s). During immobilization step, the electrode was immersed in 0.1 M Phosphate buffer (pH 5) containing desired quantity of nsDNA structures. After immobilization step, the electrode was washed with water to remove unbounded nsDNA structures and preserved at 4 °C for further use.

2.4. Electrochemical characterization of biosensor

Differential Pulse Voltammetry, Cyclic Voltammetry and Electrochemical Impedance Spectroscopy were used to electrochemically characterize the immobilized nsDNA layers over the modified electrode. DPV technique was used in order to study the oxidation of the purine

bases in 0.1M phosphate buffer at pH 7. (DPV Conditions: potential increase of 0.04V, pulse amplitude of 0.05V, pulse width of 0.017s and pulse period 0.2s). The film forming abilities and the barrier effect of DNA layer at the interface of the biosensor were studied in 10/10mM solution of $K_3Fe(CN)_6/K_4Fe(CN)_6$ in 0.1M NaCl solution using EIS and CV respectively. EIS was performed at frequency between 0.1 Hz and 1MHz in 51 frequency steps. CV was performed between +0.7 V and -0.7 V at a scan rate of 50 mV/s.

2.5. Electrochemical determination of aromatic compounds

Solutions of 16 DNA damaging aromatic compounds were prepared separately to determine their effects over all the three prepared biosensors. The DNA bases in the biosensor were allowed to react with the analyte for 5 minutes after which it was washed with distilled water to remove the excess analytes over the biosensor. The change in the electrochemical signals was recorded and the following equation was used to find the relative percentage of DNA damage due to the analyte.

$$\Delta R_{ct(rel)}\% = [(R_{ct(surv\ DNA)} - R_{ct(MWCNT)})/(R_{ct(DNA)} - R_{ct(MWCNT)})]* 100 \qquad [1]$$

The value of the binding constant for the interaction of aromatic compounds with DNA in biosensor was determined from the following equation.

$$\text{Log } (1/\text{ANALYTE}) = \log K + \log [\ (R_{ct(surv\ DNA)})/(R_{ct} - R_{ct\ (surv\ DNA)})] \qquad [2]$$

where R_{ct} is the charge transfer resistance at EIS measured at the peak potential at the modified electrodes without DNA. The indexes used, characterize the chemical modifiers of graphite electrode (Peng et al., 2007). By plotting log(1/analyte) versus log $[\ (R_{ct(surv\ DNA)})/(R_{ct} - R_{ct\ (surv\ DNA)})]$, the value of K was determined from the intercept value (Liu et al., 2008).

3. Results and Discussion

3.1. Formation of DNA nanostructure

nsDNA template was so designed that it forms a Holliday junction. A Holliday junction is a junction between four strands of DNA, named after Robin Holliday who proposed this in 1964 (Stahl, 1994). The Holliday junction is a critical intermediate in homologous genetic recombination (Duckett et al., 1988). We expected three hair pin loops, four self-dimers and one Holliday junction for the designed template. Fig. 1 displays the TEM and AFM image of ns-DNA structures and the inset displays the magnified ns-DNA structures. Individual ns-DNA structures were found to be approximately 50 nm in size. The obtained ns-DNA structure may also be termed as DNA nanostructures derived from single DNA template sequence. Once the

DNA template sequence was heated to its annealing temperature and then cooled till 58 ºC, self dimerization within the single DNA template sequence favored the formation of three hair pin loops, four self-dimers and one Holliday junction, as predicted in each treated ns-DNA structure. Self dimerization within the single sequence is quite common in GC rich regions (Wilson and Hunt, 2008). nsDNA template sequence is designed to have GC rich regions (56.2 %) so that it favors self dimerization. However, it has to be noted that due to high GC content, untreated nsDNA sequence has been noticed to form self dimmers with the neighboring DNA sequence and end up in formation of circular DNA structures of various diameters. Hence, it can be inferred that the formation of nanostructure is temperature directed self assembly.

Microscopic techniques have been commonly used to examine biological samples. In this report TEM and AFM was used to confirm the formation of nanostructures from the above mentioned procedure. Similar nanostructures can be noticed in all the insets (a) of Fig. 1. AFM image is similar to the image obtained from TEM analysis (Inset (b) of Fig. 1). The observed data confirms the formation of nsDNA structure. Also, it is predicted that the untreated DNA template forms a circular structure. This circular structure is formed when DNA template forms self dimer within the self and with the neighboring DNA templates. The self dimer bonds are broken at the annealing step, as mentioned in step 1. Later, on sudden decrease of the temperature to 58 ºC, the single stranded DNA template supercoils to form a DNA nanostructure. Further studies have to be performed to identify the nature of the supercoiling, the number of twists and writhes it forms and later how this template sequence forms a nanostructure with four arms.

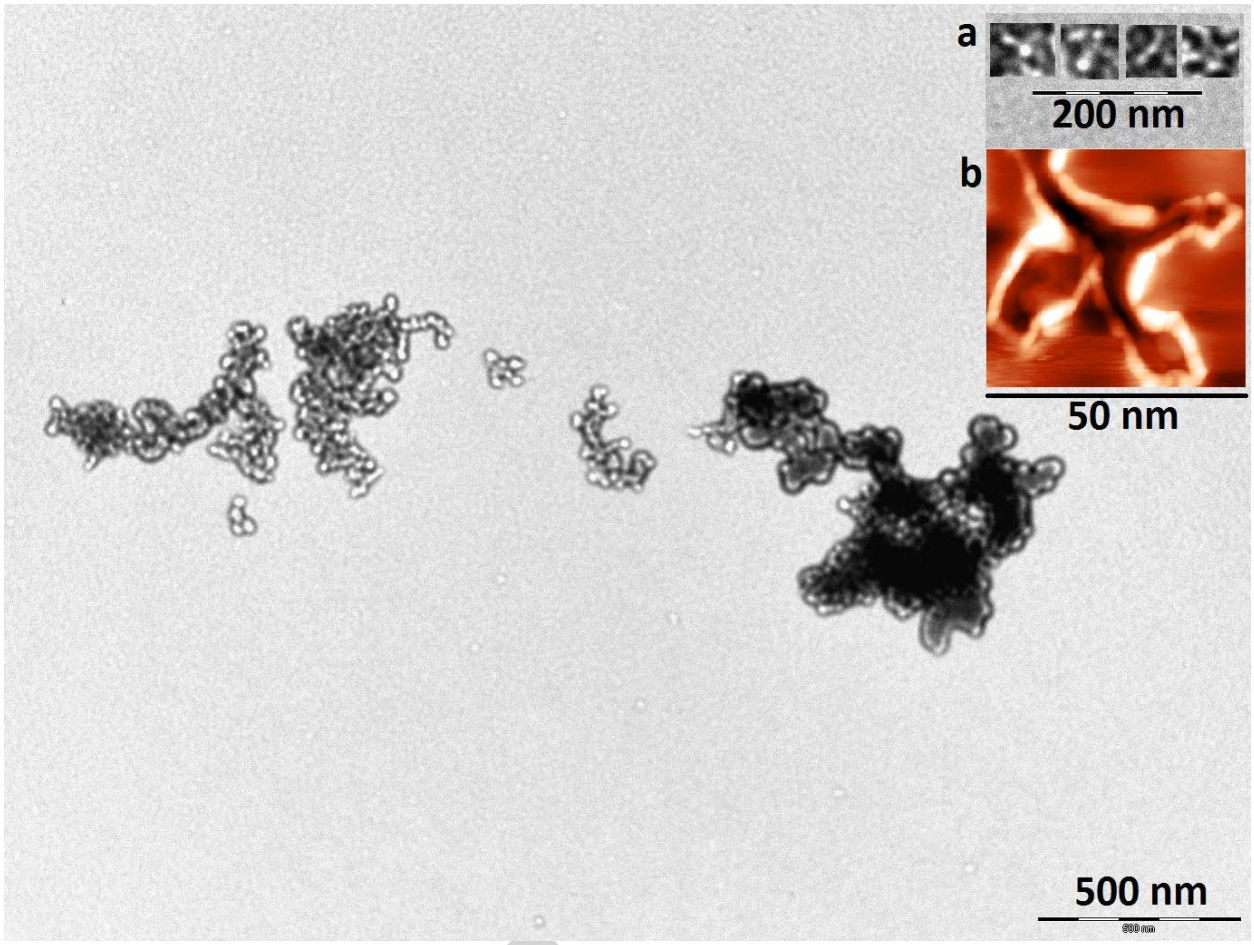

Fig. 1. TEM image of DNA nanostructure; Inset (a). Individual nanostructures obtained, Inset (b). AFM image of DNA nanostructure

3.2. Optimization of nsDNA biosensor

Schematic representation of the preparation of nsDNA based biosensor has been display in Scheme 1. Electrostatic attraction method has been adopted for the immobilization of nsDNA over the working electrode. The negatively charged backbone of phosphate group is proposed to electrostatically interact with the positively charged working electrode on applying potential of +0.3 V (versus calomel electrode).

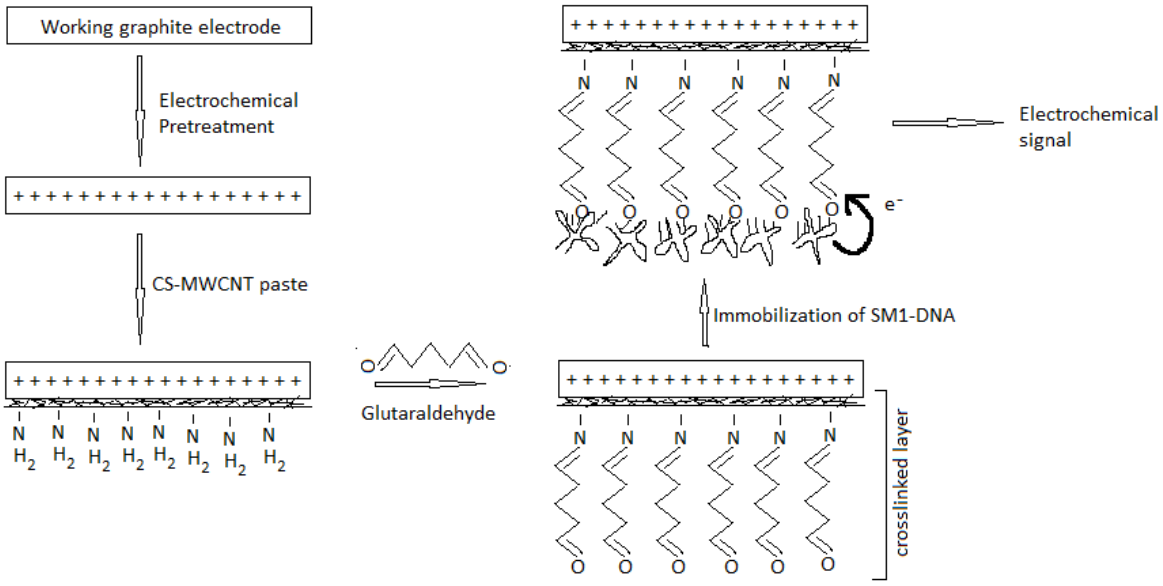

Scheme 1. Scheme of electrochemical preparation of nsDNA based biosensor

Optimization is the process of developing and implementing technical standards by identifying the exact concentration of the reaction compounds required to perform a reaction. In this report, graphite electrode is used as working electrode during electrochemical analysis. In order to enhance the electrochemical property of this working electrode, the surface of the graphite electrode is made to undergo certain modification using MWCNT, chitosan and glutaraldehyde. Biosensor with the layers of nsDNA was immobilized over modified graphite surface. Optimization was obtained when 60 mg/l of nsDNA was immobilized over modified graphite surface containing 1 mg/ml of MWCNT for 180 s (Details available in supplementary Data Sheet).

3.3. Electrochemical characteristics of DNA nanostructures

The electrochemical properties of modified graphite electrode have been discussed in detail in the earlier report of the authors. Fig. 2 represents the DPV peaks of the nsDNA immobilized over modified electrode (GTA/CS-MWCNT/G). For comparison, DPV peaks of purine nucleobases (PN), purine nucleosides (PS), single stranded DNA (ssDNA) and double stranded DNA (dsDNA) have also been displayed. This was used to show the change in oxidation signals from the bottom up approach. As we can notice that oxidation peak current of purine nucleosides are less when compared to purine nucleobases and it subsequently becomes

lesser for ss and ds DNA; and least for ns-DNA. The complexity of the structure increases with the presence of other elements which may hinder the oxidation of guanine and adenine, and is reflected in the oxidation signal during DPV analysis. Higher oxidation peak currents were observed for purine bases in ssDNA when compared to the oxidation signals observed after the addition of its complementary base. ssDNA, consists of the purine and pyramidine nucleotides covalently linked via phosphodiester bonds (Wilson and Hunt, 2008) and its bases are free to react. Where in dsDNA, the hydrogen bonds between the nucleotides and base-stacking interactions among aromatic nucleobases make the structure more rigid, influencing the oxidation of purine bases (Carlo et al., 2008). Guanine and adenine of nsDNA were found to get oxidized at 0.8 and 1.08 V respectively. The formation of more rigid and stable structure in nsDNA has resulted in the lesser oxidation peak current in comparison with ss and ds DNA containing 50 nucleobases.

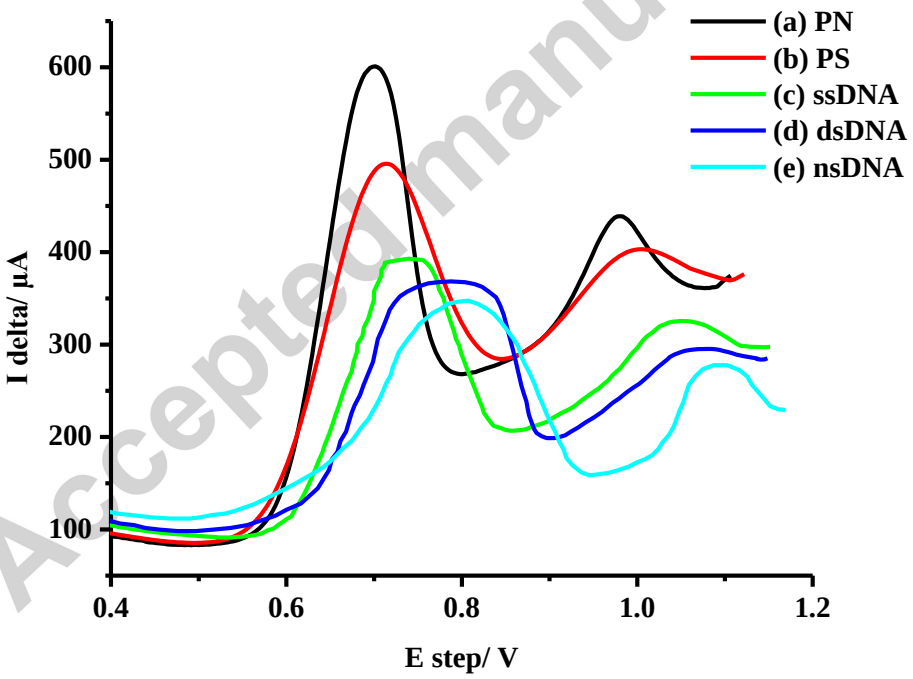

Fig. 2. Standardized DPV curves of various sensing materials over modified graphite

Further, EIS spectra for the standardized biosensors were performed. This was done to study the charge transfer characteristics of the immobilized sensing media over the modified electrode. The Nyquist plots obtained from various electrodes is represented in Fig. 3. Nyquist plots of all the samples display a semicircle at high frequencies and linear plots at low

frequencies. MWCNT coated graphite electrode shows a small semicircle (R_{ct} = 13.39 Ω) indicating excellent conductivity of MWCNT. However, on the addition of binding agents and sensing media, the electron transfer resistance increases but does not exceed the charge transfer resistance of bare graphite electrode (≈16 to 43 Ω). The impedance data was simulated using the Randles equivalent circuit consisting of a parallel combination of the capacitance (C_{dl}) and the charge transfer resistance (R_{ct}) redox reactions in series with the supporting electrolyte resistance (R_{sol}).

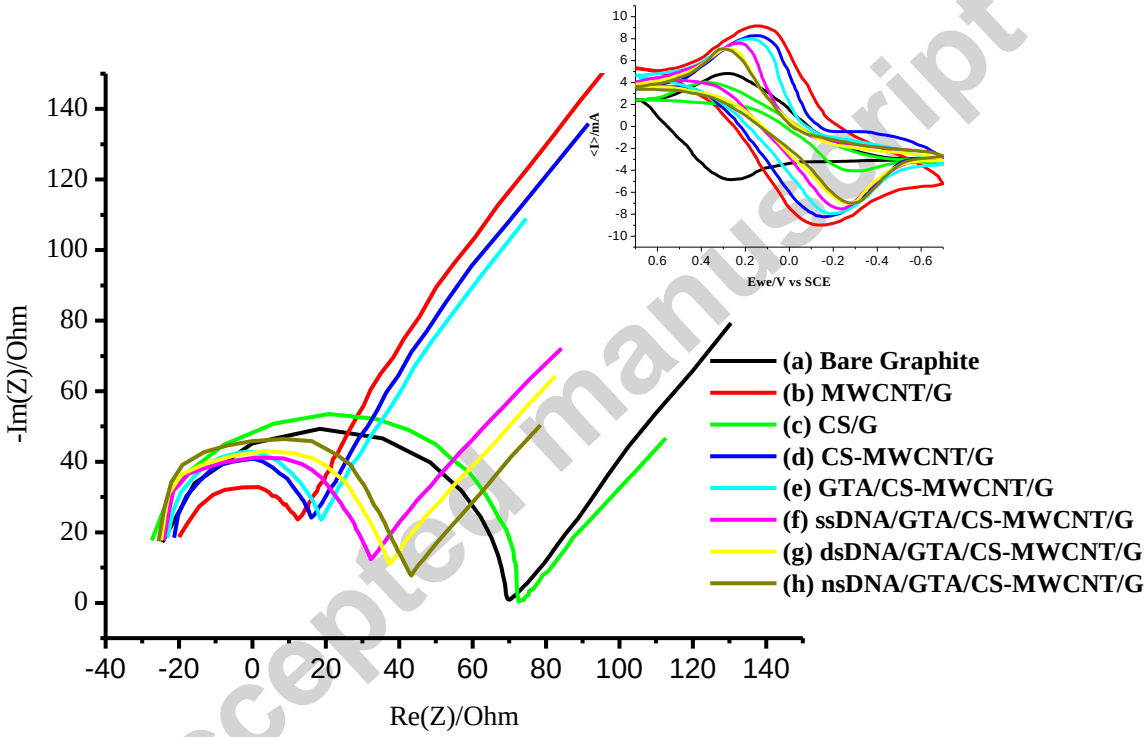

Fig. 3. The Nyquist plots obtained for optimized values of various modified electrodes; Inset: Cyclic Voltagrams obtained for optimized values of various modified electrodes

As ssDNA template was introduced to the modified electrode, the diameter of the semicircle increased and thus increasing the R_{ct} value upto 31.89 Ω. The diameter of the semicircle still increases (R_{ct} = 37.40 Ω), with the introduction of ds-DNA. Further, on the addition of ns-DNA, to GTA/CS-MWCNT/G electrode, the R_{ct} value further increases (43.27 Ω). This suggests that the electron transfer process was further blocked because of the

electrostatic repulse of $[Fe(CN)_6]^{3-/4-}$ redox ions with the increase in structural complexity of the immobilized DNAs. It was found that the R_{sol} shows a negative resistance in the Nyquist plot. Numerous examples of negative resistance have been reported and in all the cases, the condition, $Re[Z\omega]_{\omega \to 0<0}$, is associated with a passivation event in which the steady state current decreases with increasing voltage (Macdonald, 1990). In other words, the electrochemical adsorption of a blockage intermediate from the electrolyte over the working electrode is a passive event ultimately reperesented as a negative resistance. However, the charge transfer resistance is at the positive portion representing the active transport of the redox ions.

CV was performed to confirm the findings of EIS spectra. The addition of MWCNT over the graphite electrode significantly improves the electrochemical reversibility of the redox probe (ΔE_p = 0.236 V) and at the same time increases its current response (I_{pa} = 8.95 mA and I_{pc} = -8.96 mA). As the ssDNA is introduced onto the modified electrode surface, the ΔE_p (0.468 V) value increases and the cathodic peak current value decreases. The ΔE_p (0.549 V and 0.586 V) values further increases with the introduction of dsDNA and nsDNA. This is consistent with DPV and EIS findings. It has to be noticed that ΔEp, the peak potential difference between the redox peaks is theoretically 59mV and in practice, the difference is typically 70 to 100 mV. At the same time, non-symmetric redox peaks are the indications of irreversible reaction (Tissue, 2013). In all the modified electrodes (Fig. 3 Inset), ΔEp was found to be between 200 and 700 mV which is beyond the characteristic peak potential difference for reversible reaction. However, the anodic to cathodic peak current ratio is symmetric and in the range of 0.89 - 1.01, confirming the reversibility of the redox couple (Ziyatdinova et al., 2008; Gayathri et al., 2014b).

3.4. Electrochemical determination of aromatic compounds

nsDNA were attacked by exposing the modified electrodes to 16 aromatic compounds. The relative percentage of survived DNA bases was calculated from EIS, before and after the exposure. Fig. 4 display the calibration curves obtained from the average relative portion of survived bases due to prepared biosensors using EIS.

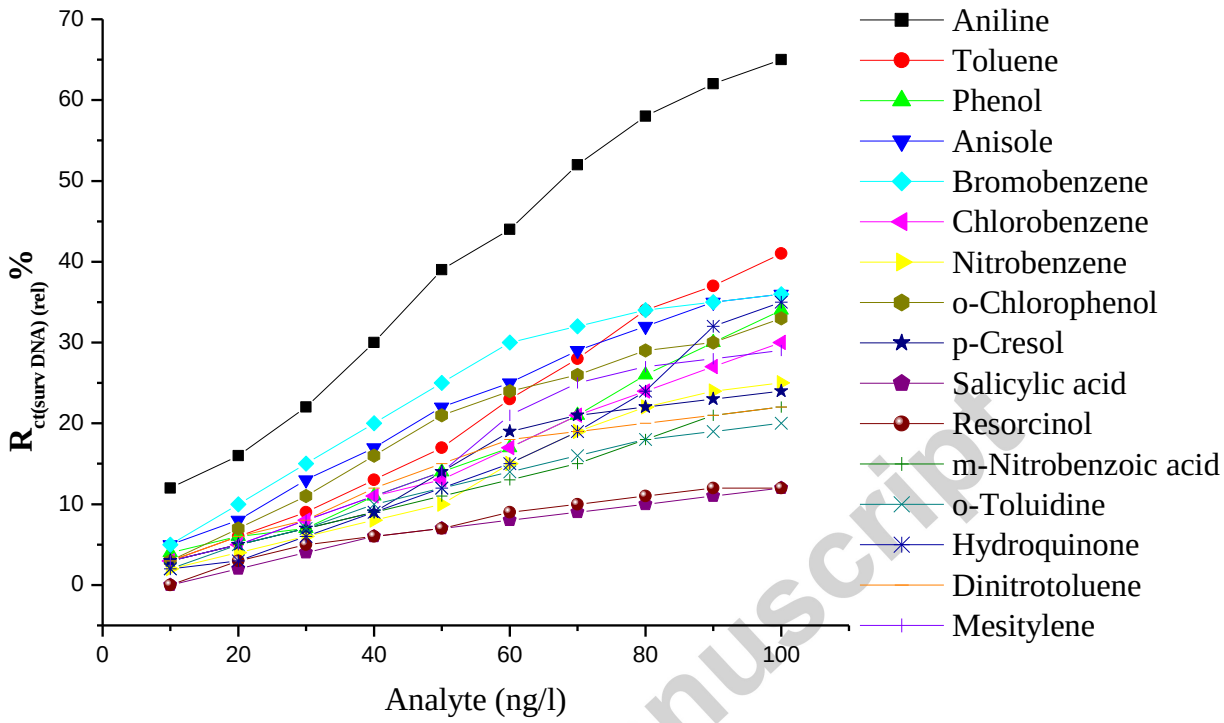

Fig. 4. Calibration curves for DNA damaging profiles obtained for nsDNA/GTA/CS-MWCNT/G biosensor for aromatic compounds

It can be noticed that apart from nsDNA, the ssDNA and dsDNA based biosensors reacted well with the exposed aromatic compounds. However, the sensitivity (6 ng/l) for the determination of aromatic compounds was high for nsDNA based biosensor. Secondly, a bottom up approach from ssDNA to nsDNA structure (ssDNA and dsDNA calibration data available in supplementary data sheet), a linear pattern for calibration was obtained. This may be due to the availability of larger interaction sites as the complexicity of the structure increases. Fitting of the linear regression data is most common and simple method for the calibration of sensing device (Aggarwal, 2013).

3.5. Electrochemical determination of biosensor-analyte binding mode

The interaction of DNA with drugs (Neault et al., 1995), ligands (Ricci and Netz, 2009) and metal complexes (Shahabadi et al., 2011) have been widely reported using various techniques including FTIR, laser Raman difference spectroscopy, fluorimetry, spectrophotometry, circular dichroism, viscosimetry, cyclic voltametry and computational

simulation. Electrochemical method is one of the techniques (Rauf et al., 2007) where the DNA-drug binding mode has been elucidated using chronopotentiometry, cyclic voltammetry, square wave voltammetry and differential pulse voltammetry. Now, the present work has made an attempt to understand the mode of binding of the 16 aromatic compounds with the implemented three DNA structures. It should be noted that the EIS spectral results bring out the change occurring in complete DNA structure whereas DPV peaks explore the changes occurring in the guanine and adenine bases in the DNA structure. The values of K are in the order of 10^8 and above for all the four DNA structures. Hence it can be inferred that these compounds could have binded strongly by non-covalent bonding. Further it may be suggested that this might have occurred at the grooves. In addition, high K values for all the four structures rule out the possibility of intercalation of the aromatic compounds to the DNA.

Hence, from the available data, it has been proposed that once DNA encounters aromatic compounds, there is a change in charge transfer resistance due to non-covalent interaction between the aromatic compounds and DNA. In the reported work, it is evident that the R_{ct} value increases after the interaction of aromatic compounds which might be ascribed to the formation of DNA adduct. It can be proposed that the DNA layer on the electrode surface enables the accumulation of aromatic compounds leading to the conformational changes in the DNA structure followed by the binding of the aromatic compounds to the DNA bases, thus altering the electrochemical signals.

3.6. Selectivity of nsDNA biosensor

Two samples were prepared manually by mixing known concentration of toluene in hexane and naphthalene and labeled as sample 1 and sample 2, respectively. All the three compounds were known constituent of gasoline. nsDNA based biosensors showed a significant response with the prepared samples, represented in table 1. It was observed that both hexane and naphthalene (simplest polycyclic aromatic hydrocarbon) did not interfere with the biosensor determination of the selected aromatic compound (Toluene) in this study. This result confirms the concept of implementing DNA nanostructures for the selective determination of aromatic compounds.

Table 1

nsDNA based biosensor determination of toluene in prepared analyte mixture

Sample	Amount of Toluene taken	Biosensor determination (n=3)
Sample 1	60	59.5
Sample 2	70	71

3.7. Real sample analysis

The biosensor response for the real samples analysis was also evaluated in order to determine the sensitivity of biosensors towards aromatic compounds during actual application. Two samples, sample 1 and sample 2 were obtained from the effluent of dye unit and that of whole industry of a tannery unit located in Pallavaram, Chennai. The obtained samples were made to react with the nsDNA biosensors. The biosensors showed a significant response towards the two samples.

3.8. Reproducibility of biosensor

Reproducibility of the biosensor was examined by determining 100 ng/L of aromatic compounds for three replicate measurements. The relative standard deviation value for the above method was found to be 1.59 %, indicating satisfactory reproducibility of the proposed biosensor. The stability of the biosensor was also evaluated by measuring the DPV response for a period of 30 days during storage. Till 26 days, there was no apparent change in the DPV signal of guanine and adenine base. Later the peak intensity of guanine and adenine was found to decrease relatively by 5 %. These observations could be attributed to the fact that nsDNA was firmly attached to GTA/CS-MWCNT/G electrode and the biosensor had a significant stability.

3.9. Comparison with UV-Visible spectroscopy

UV-visible spectroscopy was also used to investigate the interaction between nsDNA and aromatic compounds. When nsDNA and 100ng/ml of 16 aromatic compounds were mixed, the spectra were significantly different from that of nsDNA. The absorption bands (available in supplementary data sheet) of nsDNA at 200 nm showed decrease in peak intensities (hypochromicity) with aromatic compounds. Meanwhile, the band at 260 nm shifted to longer wavelength. Such a pronounced hypochromism and a bathchromism were suggested due to non-covalent bond between the nsDNA and aromatic compounds.

4. Conclusion

The change in charge transfer resistance value due to the interaction of aromatic compounds over nsDNA was investigated and calibration curves were obtained. A near linear plot was obtained during calibration for various aromatic compounds for nsDNA based biosensor in comparison with ssDNA and dsDNA based biosensor. This has paved the way of using DNA nanostructures based biosensor for selective and sensitive identification of aromatic compounds.

Acknowledgement

The authors thank the University Grants Commission (Award Letter No. F1-17.1/2011-12/RGNF-SC-TAM-143/(SA-III/Website), India for its financial support; Centralized Instrumentation Lab, Madras Veterinary College, India, for providing TEM facilities; Center for Nanoscience and Nanotechnology, Satyabhama University, India, for providing SEM and AFM facilities and SRM University, India, for providing other technical facilities to carry out this part of the research work.

References

- Aggarwal, C. C., 2013. Managing and mining sensor data, Springer Science & Business Media, New York.
- Arias, P., Ferreyra, N., F., Rivas, G., A., and Bollo, S., 2009. J. Electroanal. Chem., 634, 123-126.
- Cai, H., Xu, C., He, P., and Fang, Y., 2001. J Electroanal Chem., 510, 78-85.
- Carlo, M. D., Marcello, M. D., Perugini, M., Ponzielli, V., Sergi, M., Mascini, M., Compagnone, D., 2008. Microchim. Acta., 163, 163-169.
- Duckett, D. R., Murchi, A. I. H., Diekmann, S., Kitzing, E., Kemper, B., Lilley, D. M. J., 1988. Cell, 55, 79-89.
- Gayathri, S. B., Kamaraj, P., 2015. Chem. Sci. Trans., 2015, 4, 303-311.
- Gayathri, S. B., Kamaraj, p., Arthanareeswari, M., Devikala, S., 2014a. Chem. Sci. Trans., 3, 1446-1454.
- Gayathri, S. B., Kamaraj, P., Arthanareeswari, M., Devikala, S., 2014b. Int. J. Electrochem. Sci., 9, 6113-6123.
- Kamel, A. H., Moreira, F. T., Delerue-Matos, C., Sales, M. G., 2008. Biosens. Bioelectron., 24, 591-599.
- Liu, N., Li, G., Liu, S., Zhang, S., 2008. Sensor. Actuat. B-Chem., 2008, 133, 582-587

- Macdonald, D. D., 1990. Electrochim. Acta., 35, 1509-1525.
- Marrazza, G., Chianella, I., Mascini, M., 1999. Anal. Chim. Acta., 387, 297-307.
- Neault, J. F., Naoui, M., Tajmir-Riahi, H. A., 1995. J. Biomol. Struct. Dyn., 13, 387-397.
- Palecek, E., 1988. Anal. Biochem., 170, 421-431.
- Palecek, E., 1996. Electrocatalysis, 8, 7-14.
- Pelesko, J. A., 2007. Self Assembly: The science of things that put themselves together, CRC Press, Florida.
- Peng, H., Soeller, C., Vigar, N. A., Caprio, V., Travas-Sejdic, J., 2007. Biosens. Bioelectron., 2007, 22, 1868-1873.
- Rauf, S., Nawaz, H., Akhtar, K., Ghauri, M. A., Khalid, A. M., 2007. Biosens. Bioelectron., 22, 2471-2477.
- Ricci, C. G., Netz, P. A., 2009. J. Chem. Inf. Model., 49, 1925-1935.
- Shahabadi, N., Mohammadi, S., Alizadeh, R., 2011. Bioinorg. Chem. Appl., ID: 429241.
- Stahl, F. W., 1994. Genetics, 138, 241-246.
- Tissue, B. M., 2013. Basics of Analytical Chemistry and Chemical Equilibria, John Wiley & Sons, New Jersey.
- Wilson, J. H., Hunt, T., 2008. Molecular Biology of the Cell, Garland Science, New York.
- Ziyatdinova, G., Galandova, J., Labuda, J., 2008. Int. J. Electrochem. Sci., 3, 223-235.

Highlights:

1. Simple two step procedure for the formation of DNA nanostructure from a single DNA template sequence is demonstrated.
2. Electrochemical properties of DNA nanostructures have been discussed and compared with that of single stranded and double stranded DNA.
3. DNA nanostructures immobilized over modified electrode were made to interact with DNA damaging aromatic compounds and calibration curves were obtained.